Automating Treatment Planning in Radiation Therapy

Olalekan Ogunmolu

Perelman School of Medicine
University of Pennsylvania, Philadelphia, PA

Presented by **Lekan Molu** (`Lay-con Moh-lu`)

March 10, 2021

Funding Sources

NIH NATIONAL CANCER INSTITUTE

THE STATE OF TEXAS

CANCER PREVENTION & RESEARCH INSTITUTE OF TEXAS

Talk Outline

- Beam Orientation Optimization (BOO)
  - Monte Carlo Tree Search and Neuro-Dynamic Programming for BOO
  - Column Generation as Pretraining for MCTS for BOO
- Patient Head Motion Correction in External Beam Radiation Therapy (RT)
  - Intensity-Modulated RT (IMRT): Earlier PhD Work
  - Magnetic Resonance Imaging and Linear Accelerator Systems (MRI-LINACs)
- Robustness Margins and Robust Deep Policies for Nonlinear Control

Research Significance

2021 → 1,898,160 U.S. cancer cases[1] → 608,570 deaths → $246 billion in costs by 2030[1]

Cancer Treatment

- Chemotherapy/Radiosurgery.
- Radiation Therapy (RT).

RT Signif.

- Approx. 40% of all curative cancer treatment modality are performed with RT[1].
- Cost-effective -- accounting for only 5% of the total cost of cancer care[3].

Imaging

- CT images in RT = Low soft tissues contrast ⇒ OARs toxicity during treatment planning.
- MRI of brain, and head and neck (H&N) cancers provides exceptional soft tissues contrast and allows greater delineation of cancerous from non-cancerous tissues.

IMRT Treatment Planning (Beam Delivery)

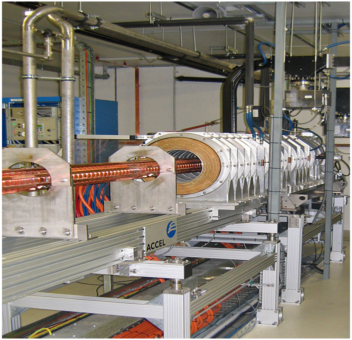

The Australian Synchrotron.

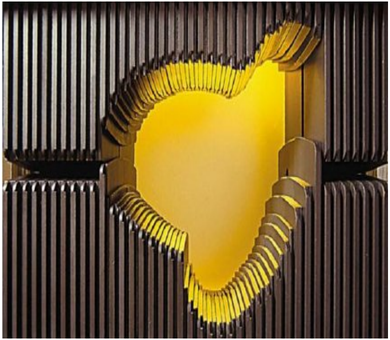

A Multi-leaf collimator, ©Varian.

Radiation Delivery Couch and Gantry

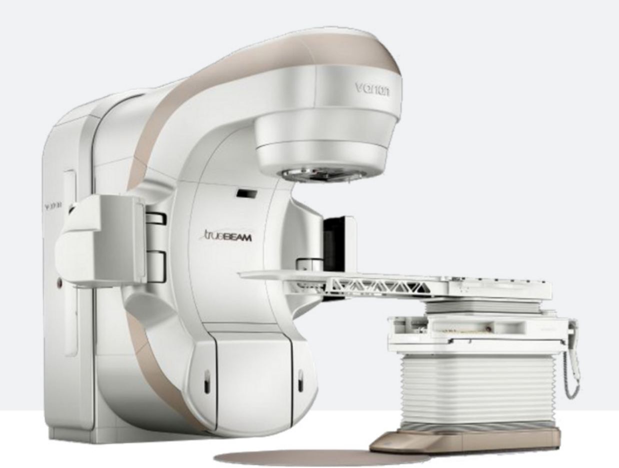

Varian's TrueBeam Radiotherapy System.

Part I.A: Beam Orientation Optimization (BOO)

- Beam Orientation Optimization (BOO)
  - Monte Carlo Tree Search and Neuro-Dynamic Programming

Contributions

Relevant Publications

Ogunmolu, Olalekan, Michael Folkerts, Dan Nguyen, Nicholas Gans, and Steve Jiang. "Deep BOO! Automating Beam Orientation Optimization in Radiation Therapy." In *Algorithm Foundations of Robotics XIII*, Merida, Mexico. Published in *Springer's Proceedings in Advanced Robotics (SPAR) Book*, 2020.

- A sparse tree lookout strategy for games with large state spaces guides transition between beam angle sets
- Tree lookout strategy guided by a deep neural network policy

Protate Cancer Example

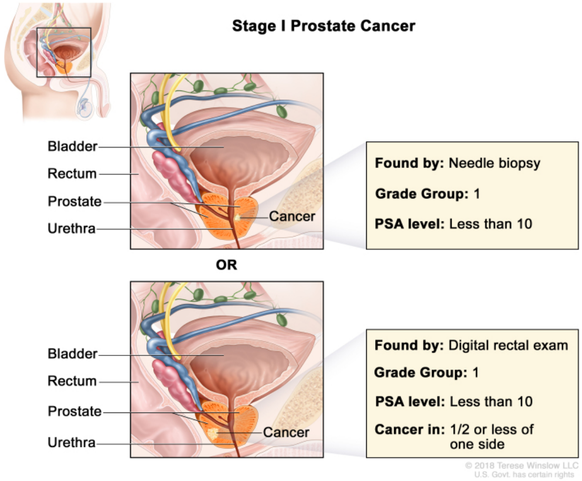

BOO Process: Fluence Map Optimization

Prostate CT slice

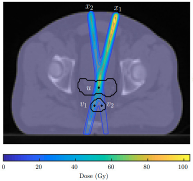

Prostate before BOO

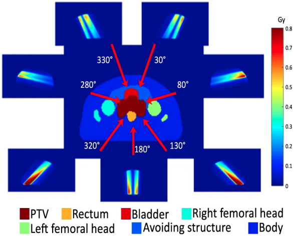

Fluence Map

BOO Workflow

Manually Selection/Protocols Adoption

Laborious process; could take up to 5 days for head and neck cancer treatment.

Pre-solve Large Sparse Dose Influence Matrix

Takes hours to solve for a single patient. Days/months for multiple patients.

Solve Fluence Map Optimization

Time-consuming: Often takes minutes.

Treatment Plan Flowchart

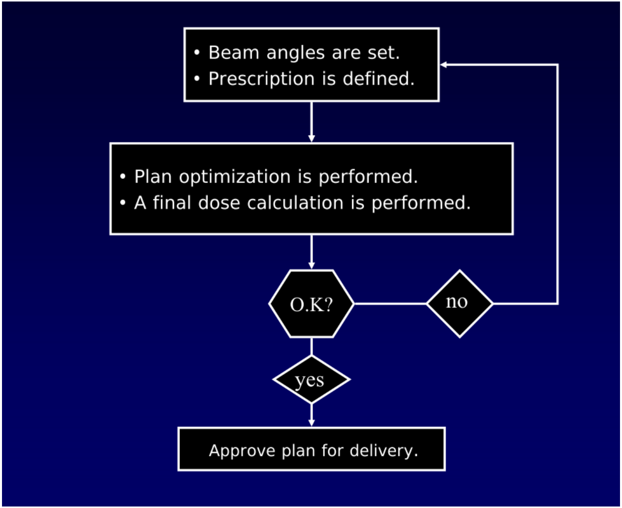

Reprinted from "IMRT Optimization Algorithms. David Shepard. Swedish Cancer Institute. AAPM 2007."

Current Approaches and Limitations

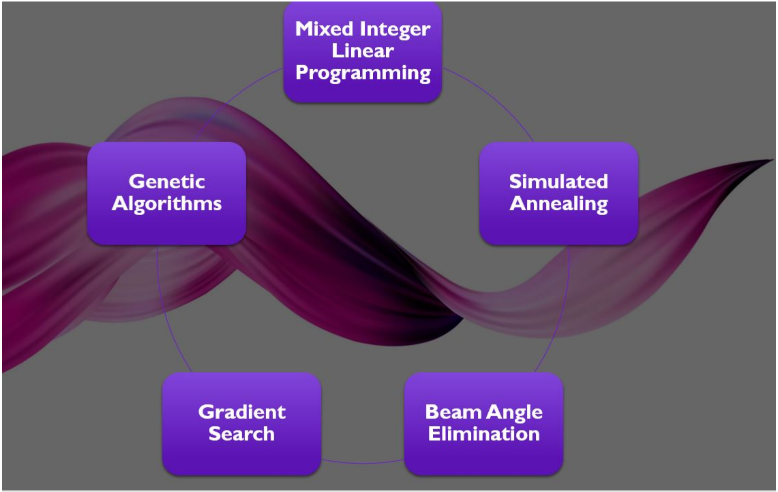

Innovation

- A Tower Neural Network generates a policy that guides MCTS simulations for two players in a zero-sum Markov game
  - Produces a *utility (value) function* & a subjective *probability distribution*
- Each player in a two-player Markov game finds an alternating best response to the current player's average strategy
  - driving the neural network policy's weights toward an approximate **saddle equilibrium** [Heinrich et al. (2015)].
  - aids network in finding an *approximately optimal* beam angle candidate set that meets a dosimetric requirements.

State Encoding: Prostate Organ Masks

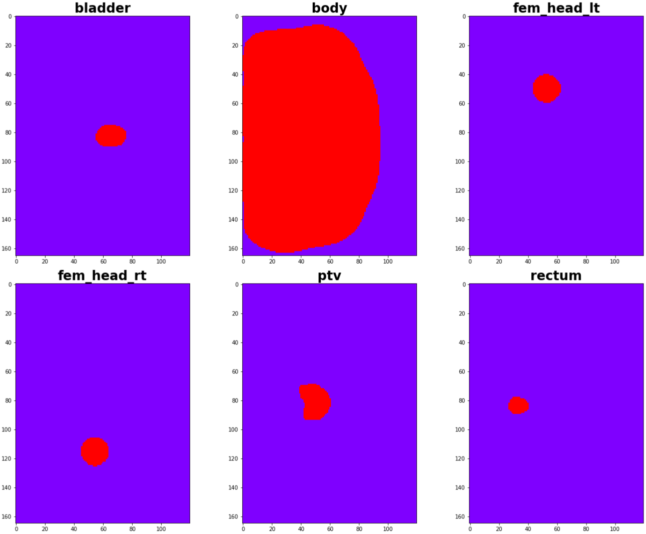

State Representation: Beam Angles

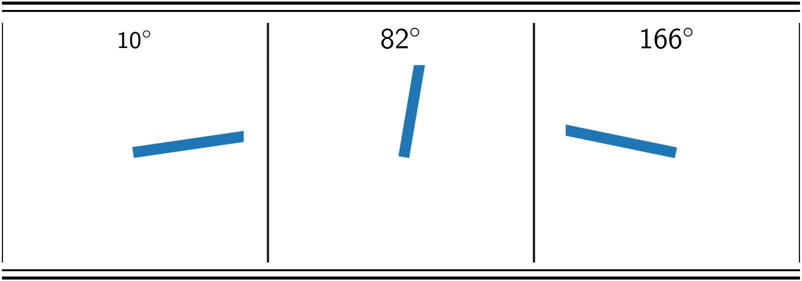

State Representation

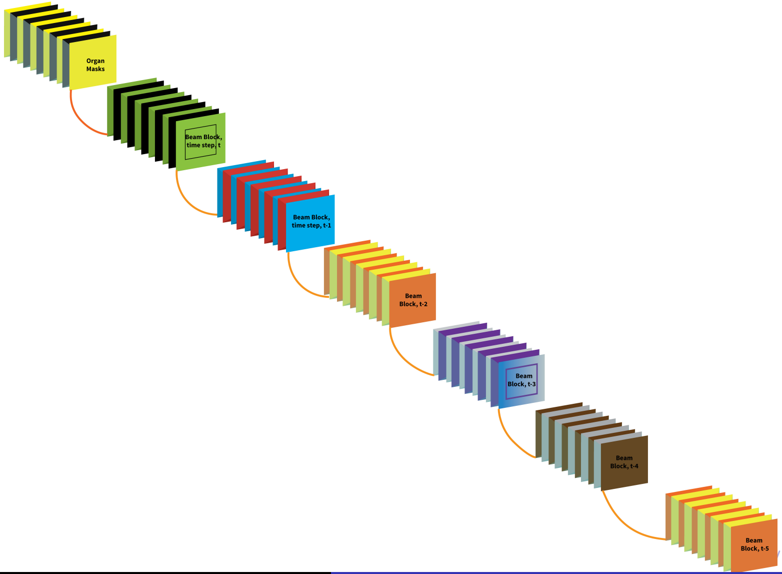

Two-player Fictitious network play with ResNet

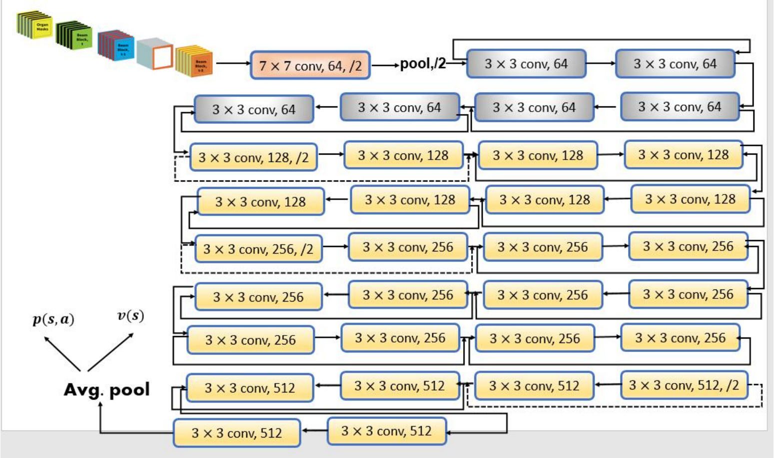

Tree Representation and Game Simulation

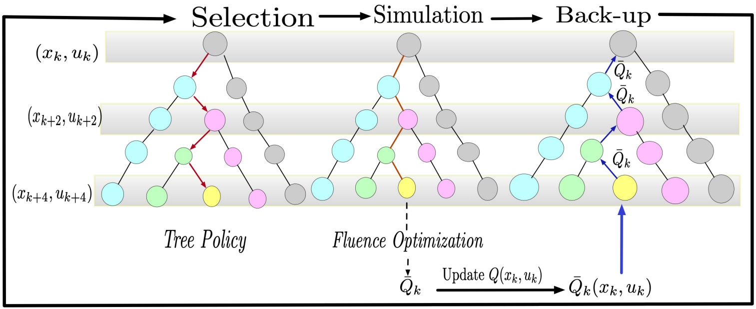

Tree Composition

Every **node** of the tree, $\boldsymbol{x}$, has the following fields:

- a pointer to the parent that led to it, $\boldsymbol{x}.p$;
- the beamlets, $\boldsymbol{x}_b$, stored at that node; $b = \{1, \ldots, m\}$;
- a set of move probabilities prior, $p(s, a)$;
- a pointer $\boldsymbol{x}.\boldsymbol{r}$, to the reward r_t, for the state $\boldsymbol{x}_t$;
- a pointer to the state-action value $Q(s, a)$ and its upper confidence bound $U(s, a)$;
- a visit count $N(s, a)$, that indicates the number of times that node was visited; and
- a pointer $\boldsymbol{x}.child_i$ to each of its children nodes.

Saddle Point Strategy Formulation

- **Saddle point strategies** for optimal control sequence pair $\{a_t^{p_1^*}, a_t^{p_2^*}\}$ recursively obtained by optimizing, $V_t(s, a)$

$$V_t^*(s) = Q_t^*(s_t, \pi_t^{p_1}, \pi_t^{p_2}) = \min_{\pi^{p_1} \in \Pi^{p_1}} \max_{\pi^{p_2} \in \Pi^{p_2}} Q_t^\star(s_t, \pi^{p_1}, \pi^{p_2})$$
$$\forall s_t \in \mathcal{S}, \pi^{p_1} \in \Pi^{p_1}, \pi^{p_2} \in \Pi^{p_2}.$$

such that

$$v_{p_1}^\star \le v^\star \le v_{p_2}^\star \quad \forall \{\pi_t^{p_1}, \pi_t^{p_2}\}_{0 \le t \le T}.$$

- p_1, p_2 respectively generating a **mixed strategy** via **averaging the outcome** of individual plays.

Training and Validation Loss

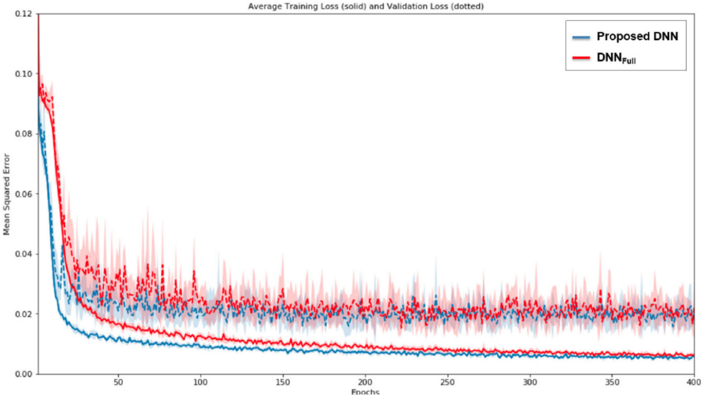

Average training (solid) and validation (dotted) loss function (MSE) values across six cross-validation folds for the network (blue) and full network.

BOO Results: Testing of self-play network

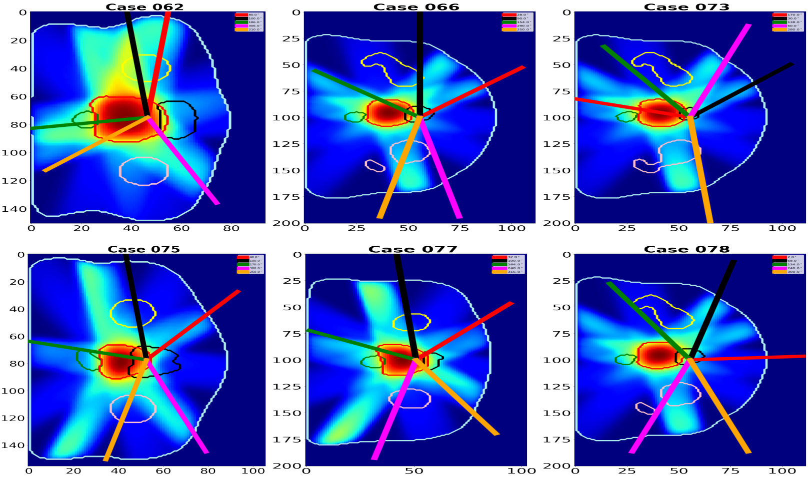

Column Generation vs Neural Network

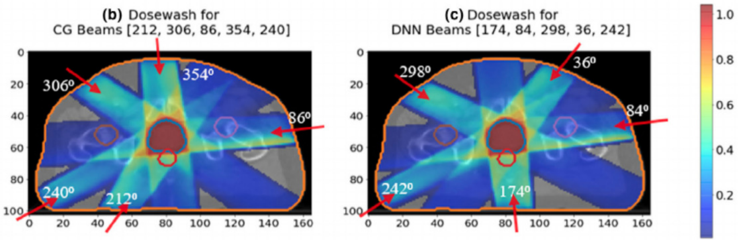

Dose-Volume Histogram of CG vs DNN architectures [Sadeghnejad Barkousaraie, Azar and Ogunmolu, Olalekan and Jiang, Steve and Nguyen, Dan (2019)].

Conclusions

- Deep Neural Network optimizes network weights in a separate multiprocessing thread; Network outputs probabilities used to guide search;
- Sparse lookahead search builds tree with nodes labeled by state-action pairs in an alternating manner; sample rewards stored on edges connecting state-action with state nodes;
- Beam angles prediction takes between 2-3 minutes with MCTS vs. ~ 60 seconds with Column Generation Pre-training.

Head Stabilization in Radiation Therapy (RT)

- Head Stabilization in Cancer Radiation Therapy
  - Intensity-Modulated RT (IMRT)

Robotic Radiosurgery

Penn
UNIVERSITY *of* PENNSYLVANIA

A Patient Head Motion-Correction Mechanism for MRI-LINAC RT

OLALEKAN OGUNMOLU
DEPARTMENT OF RADIATION ONCOLOGY, PENN SCHOOL OF MEDICINE

- Current Collaborators: Rodney Wiersma & Xinmin Liu (UChicago → UPenn)
- Past Collaborators: Steve Jiang, Xuejun Gu, (UT Southwestern); Nick Gans (UT Dallas, UT Arlington)

Correcting Head Motion: RT and MRI-LINACs

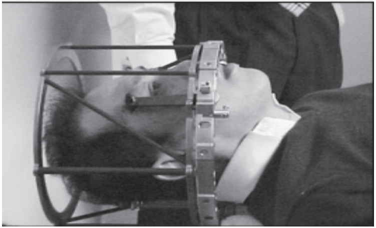

(a) The BRW SRS Frame [Chelvarajah et al. (2004)]

(b) Thermoplastic masks

(c) Frame With MRI Coils (PSOM)

4-D Motion Correction Stage

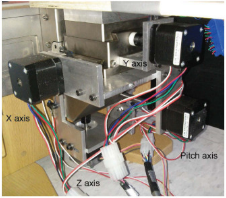

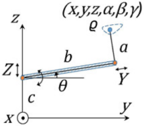

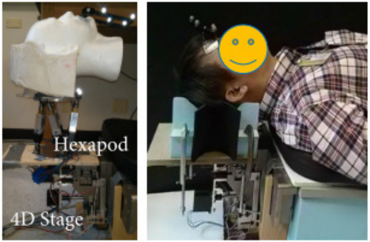

Liu et al. (2015)

4-DOF Motion Controller Block Diagram

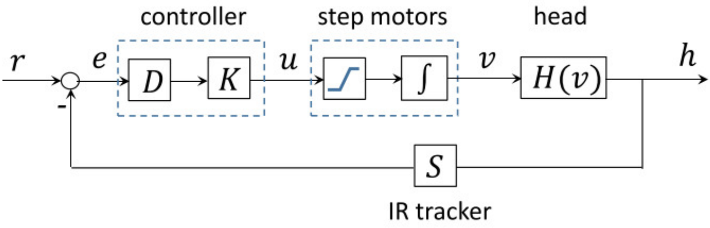

Liu et al. (2015)

Phantom Feedback Motion Correction Results

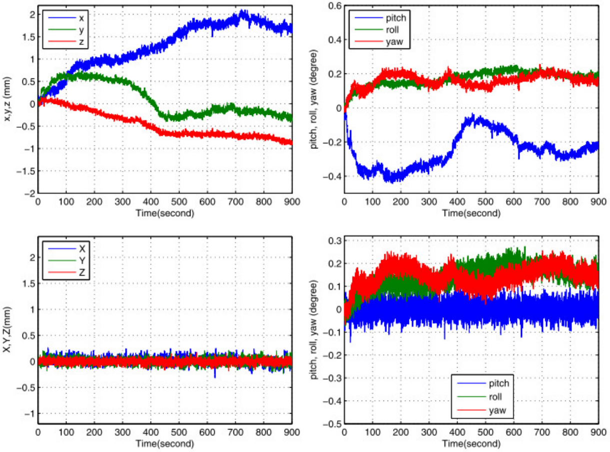

Time response of feedback control without (left) and with (right) decoupling control [Liu et al. (2015)].

Human Volunteer Feedback Motion Correction Results

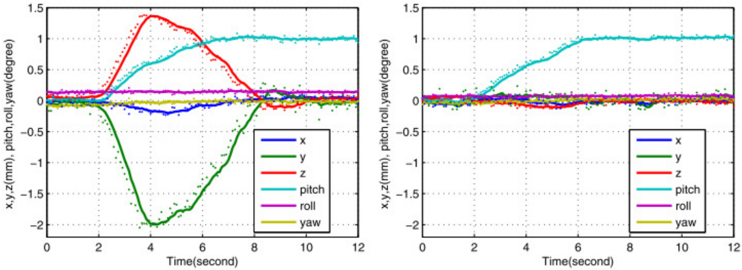

Head Motion Without and With Motion Correction. Left: Coupled Axes; Right: Decoupled Axes.

SRS: Wiersma Stewart-Gough Platform

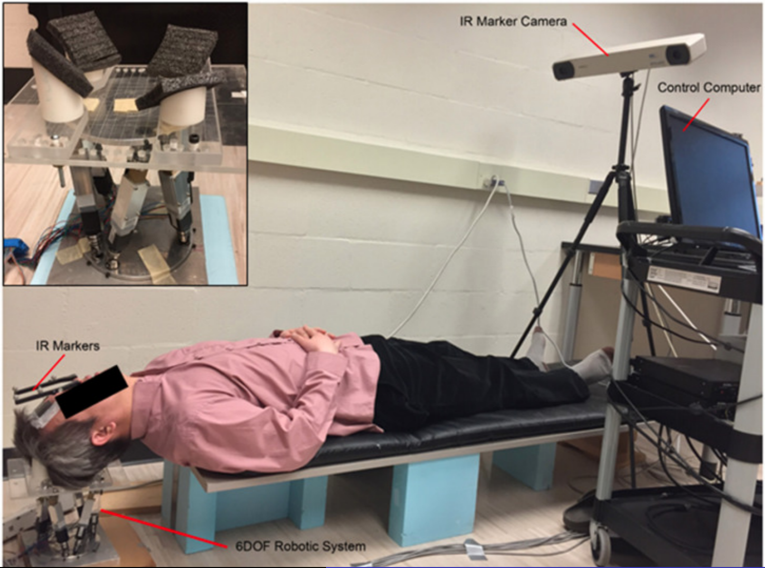

6-DOF Motion Correction Results

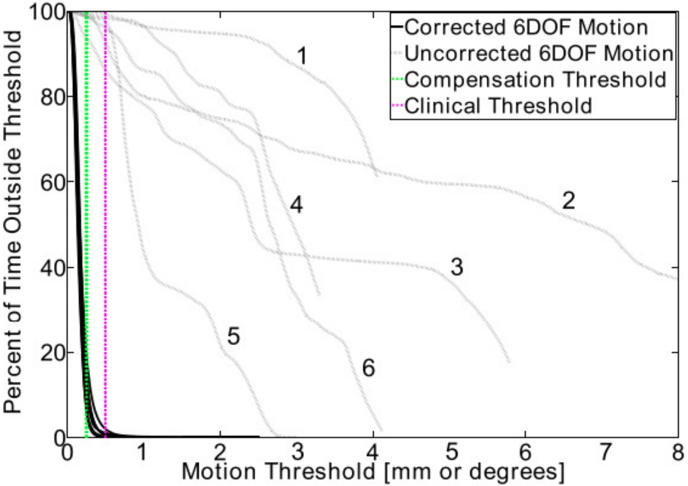

Drawbacks of current solutions

- Rigid patient's body assumption
- Non-compliant immobilization devices
- Invasiveness during radiosurgery/RT
- Attenuation of photon beams

Radiation Delivery Couch and Gantry

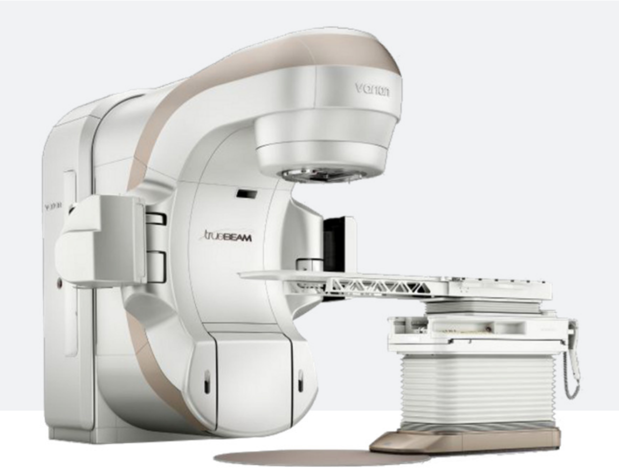

Varian's TrueBeam Radiotherapy System.

Next-Gen RT Treatment with MRI-LINACs

Elekta AB's (Sweden)

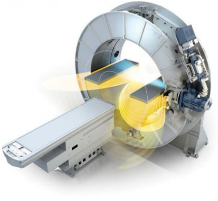

ViewRay's MRIdian

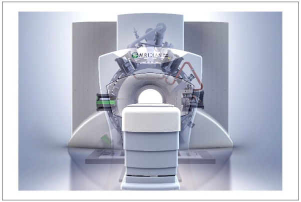

Elekta AB's (Sweden)

MagnetΓx (Canada) Aurora RT

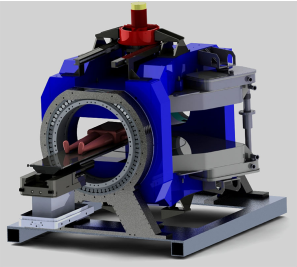

Soft Robots for Head Motion Compensation

IMRT Setup

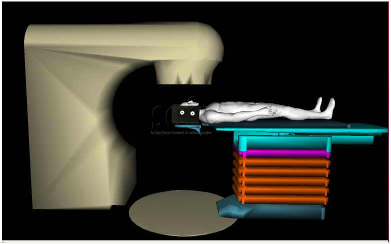

IMRT/MRI

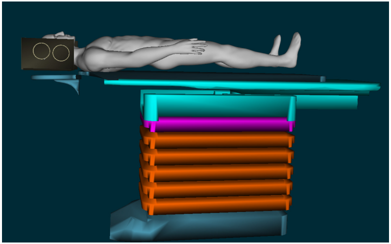

Head and Robot Panel

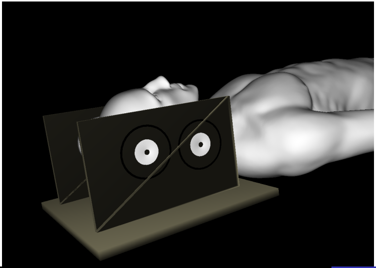

Head-Robot Closeup

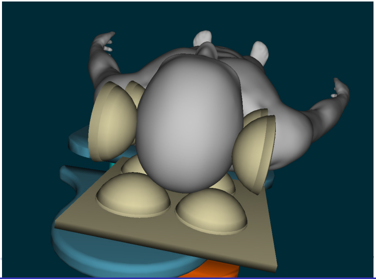

Morphing in Cephalopods

Morph Stage 1

Morph Stage 2

Morph Stage 3

Morph Stage 4

Morph Stage 5

Morph Reversal

Cephalopods Neural-Controlled Physical Texture

Raises Periscope

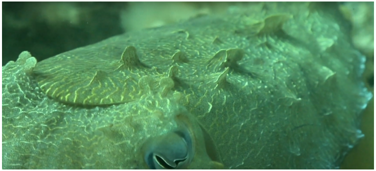

Papillae

Papillae Up

Papillae × Papillae

Cuttlefish' Morphin ©Roger Hanlon, YouTube.

Cephalopods-inspired Actuator Design

Circumferentially Constrained And Radially Symmetric Elastomers (CCOARSE).

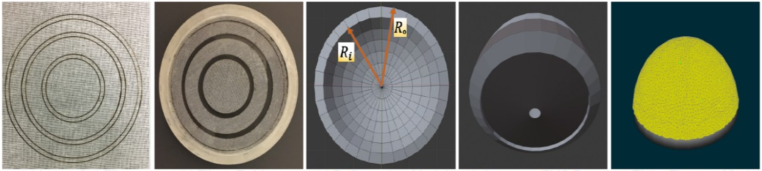

(a) Laser-Cut Fiber (b) Fiber+Rubber (c) Deformation Model (d) Actuator+PVC Base (e) Finite Element Model

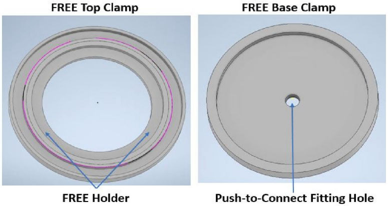

(f,g)

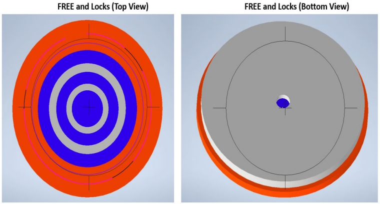

(h)

[Pikul et al. (2019)]

Nonlinear Elastic Deformation Analysis

IAB SHELLS AND AIR CAVITY/DEFORMATION ANALYSIS

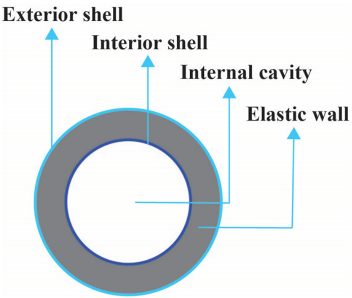

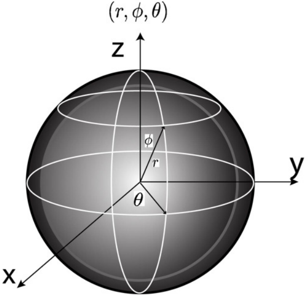

$r_i \leq r \leq r_o, \quad 0 \leq \theta \leq 2\pi, \quad 0 \leq \phi \leq \pi$

Soft IK via Boundary Value Problem

- With Cauchy's laws of motion, solve boundary volume problem of traction, and find that

$$P(r) = \int_{r_i}^{r_0} \left[2C_1 \left(\frac{r}{R^2} - \frac{R^4}{r^5} \right) + 2C_2 \left(\frac{r^3}{R^4} - \frac{R^2}{r^3} \right) \right] dr \tag{1}$$

- *i.e.* Given a prescribed radius, find pressure to deform actuator between configurations

Volumetric Deformation Results (Simulation)

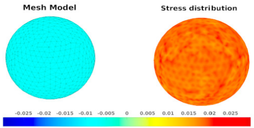

(a) **Left**: Mesh model. **Right**: Stress distribution on outer skin.

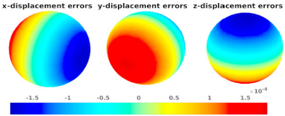

(b) Displacement errors along x, y, z coordinates.

Inputs					Outputs		
C_1	C_2	R_i	r_i	R_o	r_o	P	ΔV
$1.1e4$	$2.2e4$	$.027$	$.03$	$.03$	$.033$	$.76$	≈ 0

Fig. 6: Volumetric Deformation (Expansion).

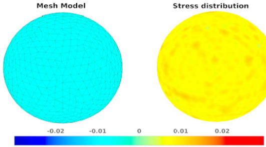

(a) **Left**: Mesh model. **Right**: Stress distribution on outer skin.

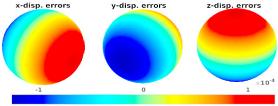

(b) Displacement errors along x, y, z coordinates.

Inputs					Outputs		
C_1	C_2	R_i	r_i	R_o	r_o	P	ΔV
$1.1e4$	$2.2e4$	$.025$	$.03$	$.03$	$.028$	$-.34$	≈ 0

Fig. 7: Volumetric Deformation (Compression).

Pneumatic Control and Deformation Scheme

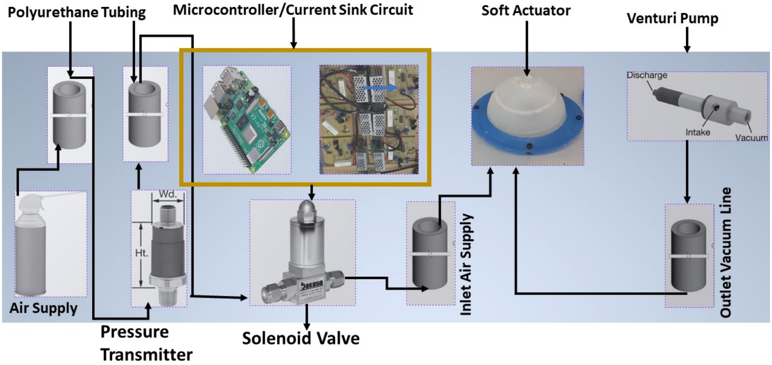

Volumetric Deformation Results (Actual)

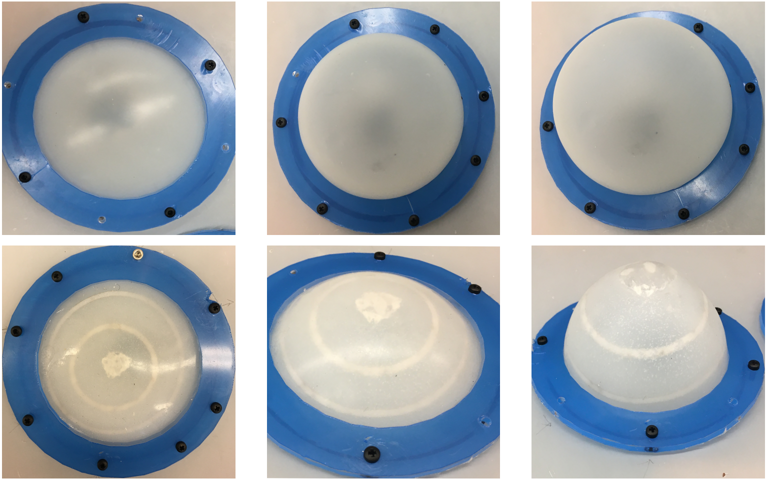

Actuator and Overall Mechanism with Phantom

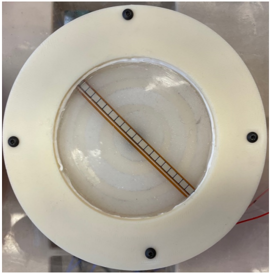

Head Motion Open Loop Control

Independent Actuation

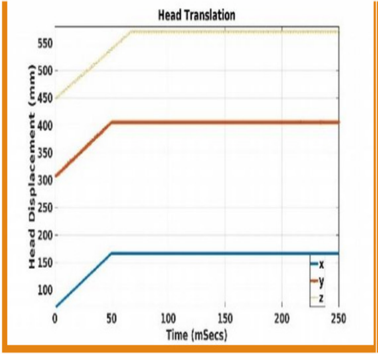

Head Translation along x, y, z for a task of raising the head by a certain threshold above the table

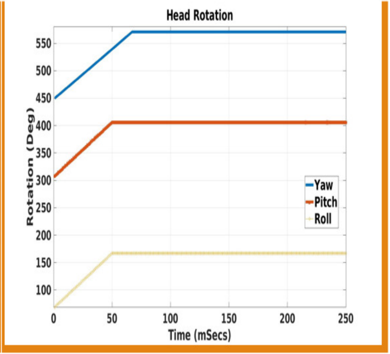

Head rotation in Euler angles for a task of tilting the head about the x, y, z axes on the treatment table.

Ongoing Work: 6-DOF Closed-loop Control

Continuum Mechanical Model Validation/Differential Geometry/Newton-Euler Dynamics

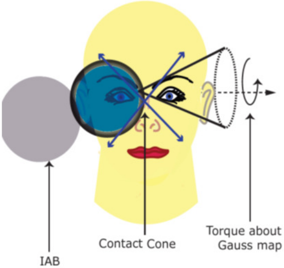

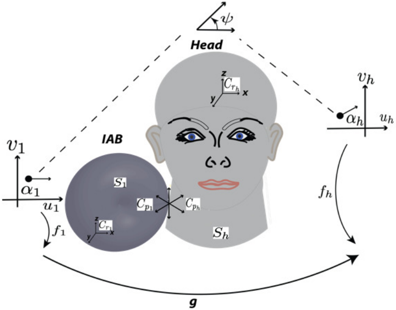

3-DOF Simulation Testbed

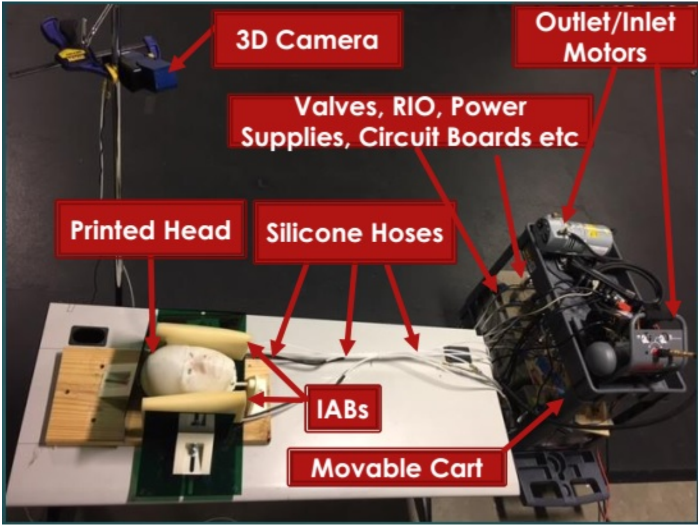

Model Reference Adaptive Control

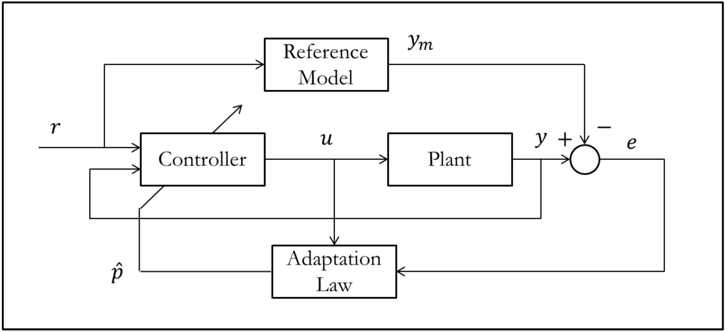

Indirect MRAC system. (Source mdpi.com)

3-DOF Model Reference Adaptive Control

- Model head and bladder dynamics as
  - $\dot{\boldsymbol{x}} = \mathbf{A}\boldsymbol{x} + \mathbf{B}\Lambda\left(\mathbf{u} - f(\boldsymbol{x}, \mathbf{u})\right) + \mathbf{w}(k)$
- Approximate $f(\boldsymbol{x}, \mathbf{u})$ by a neural network with continuous memory states
- Derive adaptive adjustment mechanism from Lyapunov analysis for Adaptive Control Parks (1966)
- $\mathbf{u} = \underbrace{\hat{\mathbf{K}}_x^{\mathbf{T}}\boldsymbol{x}}_{\text{state feedback}} + \underbrace{\hat{\mathbf{K}}_r^{\mathbf{T}}\mathbf{r}}_{\text{optimal regulator}} + \underbrace{\hat{f}(\boldsymbol{x}, \mathbf{u})}_{\text{approximator}}$

Neural Network Architecture

Neural Net Architecture

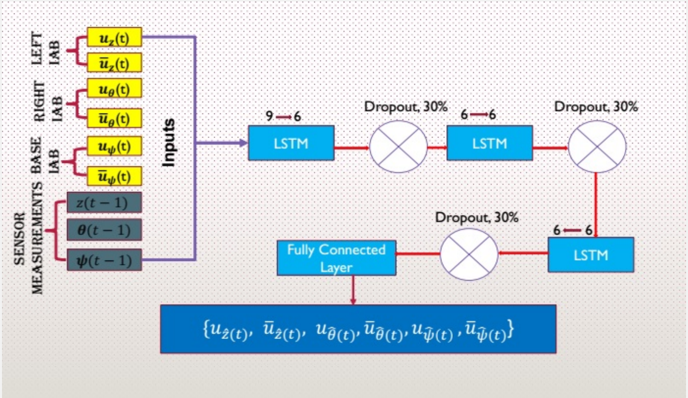

Lyapunov Redesign: Theorem

- For correct adaptive gains, $\hat{\mathbf{K}}_x$ and $\hat{\mathbf{K}}_r$, $\mathbf{e}(k)$ is ***uniformly ultimately bounded***, and the state $\boldsymbol{x}$ converges to a neighborhood of $\mathbf{r}$.
- Choose a $\mathbf{V}$ in terms of $\mathbf{e}$; $\tilde{\mathbf{K}}_x^T$, $\tilde{\mathbf{K}}_r^T$; and parameter error $\varepsilon_f(\boldsymbol{x}(k))$ space

$$\mathbf{V}(\mathbf{e}, \tilde{\mathbf{K}}_x, \tilde{\mathbf{K}}_r^T) = \mathbf{e}^T\mathbf{P}\mathbf{e} + \mathbf{tr}(\tilde{\mathbf{K}}_x^T \boldsymbol{\Gamma}_x^{-1} \tilde{\mathbf{K}}_x^T |\boldsymbol{\Lambda}|) + \mathbf{tr}(\tilde{\mathbf{K}}_r^T \Gamma_r^{-1} \tilde{\mathbf{K}}_r |\boldsymbol{\Lambda}|)$$

Results: Z and Pitch Motions

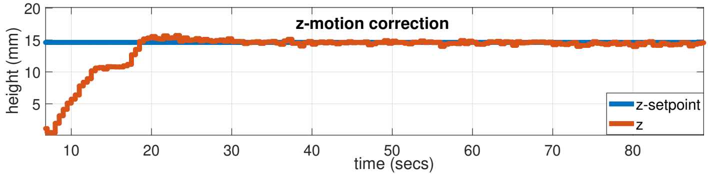

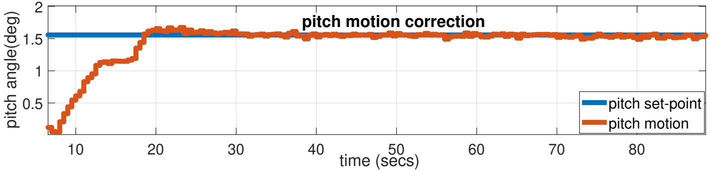

Goal command: $(z, \theta, \phi) = (14mm, 1.6^\circ, 45^\circ)^T$.

Results: Roll Motion

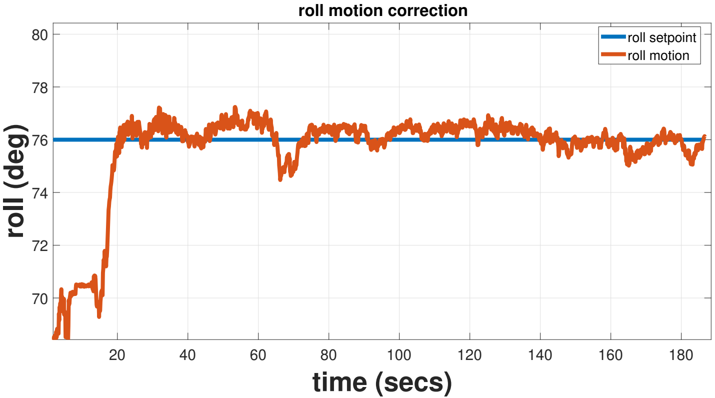

Head roll tracking.

Conclusions

- Non-invasive soft robot for head motion compensation ✓
- Photons-transparent as opposed to rigid/electro-mechanical devices/robots ✓
- Adaptible under MRI coils for newer MRI-LINACs ✓

Part III: Robustness Margins and Robust Deep Policies

- Robustness Margins and Robust Deep Policies for Nonlinear Control

The robustness conundrum

- How to know *a priori* a policy's robustness limits?

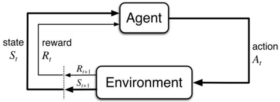

- How to inculcate robustness into multistage decision policies?

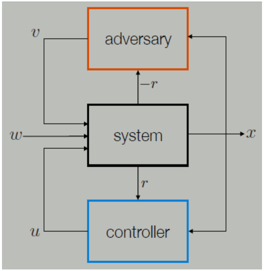

Innovation

- To quantify the brittleness, we optimize the stage cost

$$\max_{\mathbf{v}_t \sim \psi \in \Psi} \left[\sum_{t=0}^{T} \underbrace{c(\boldsymbol{x}_t, \mathbf{u}_t)}_{\text{nominal}} - \gamma \underbrace{g(\mathbf{v}_t)}_{\text{adversarial}} \right]$$

- To mitigate lack of robustness, we optimize the *cost-to-go*

$$\mathcal{J}_t(\boldsymbol{x}_t, \pi, \psi) = \min_{\mathbf{u}_t \sim \boldsymbol{\pi}} \max_{\mathbf{v}_t \sim \psi} \left(\sum_{t=0}^{T-1} \ell_t(\boldsymbol{x}_t, \mathbf{u}_t, \mathbf{v}_t) + L_T(\boldsymbol{x}_T) \right),$$

- and seek a saddle point equilibrium policy that satisfies

$$\mathcal{J}_t(\boldsymbol{x}_t, \pi^*, \psi) \leq \mathcal{J}_t(\boldsymbol{x}_t, \pi^*, \psi^*) \leq \mathcal{J}_t(\boldsymbol{x}_t, \pi, \psi^*),$$

Results: Brittleness Quantification

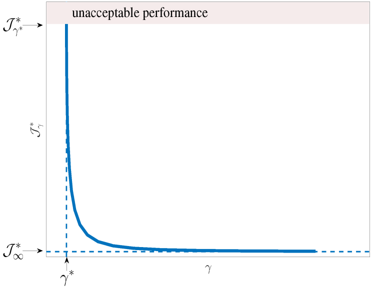

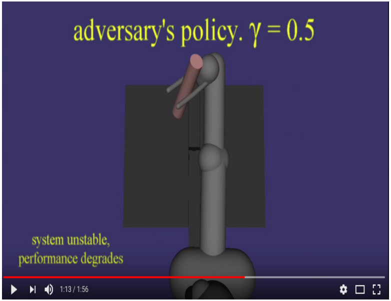

Results: Iterative Dynamic Game

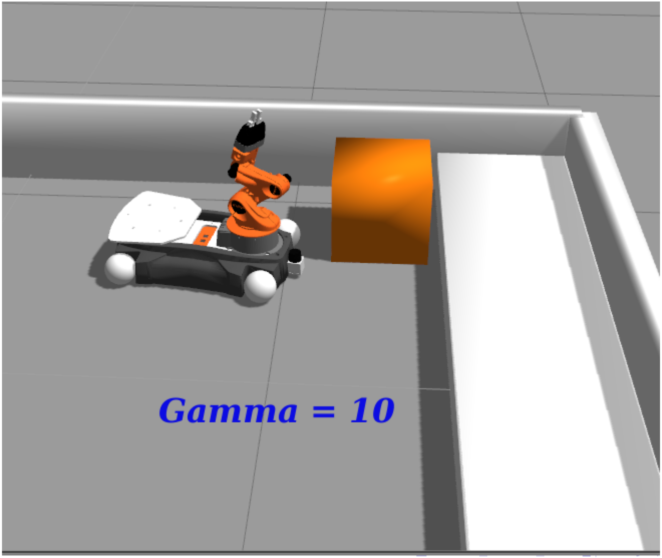

Future Work: MRI/RT Immobilization

- Explore multiple parallel robot mechanisms for head motion correction.
- Adopt iterative dynamic game approach [Ogunmolu et al. (2018)] for solving robust controller for head stabilization.
- Build on Freeman and Kokotovic's point-wise min-norm robust control lyapunov function to realize a meaningful value function in deep policies [Freeman and Kokotovic (1996)].

Constrained Robust Control Lyapunov Function (RCLF) Motion Planning

Problem Definition

Find RCLF collision-free path $\sigma^\star : [0,1] \to \mathcal{M}_{free}$ given a path planning problem $\left(\mathcal{Q}_{free}, \xi_i, \mathcal{Q}_{goal}\right)$, manipulation constraint, G, and cost function V such that $V(\sigma^\star) = \min_{\sigma \in \Sigma_{\mathcal{M}_{free}}} V(\sigma)$ if one exists.

- Leverage [Freeman and Kokotovic (1996),Ogunmolu et al. (2018)].
- Greedy approach using L-BFGS optimization algorithm with box constraints, in contrast to the quadratic nonlinear constrained optimization e.g. Khansari-Zadeh and Billard (2014).

Reproducing a Nonlinear Motion with GMM

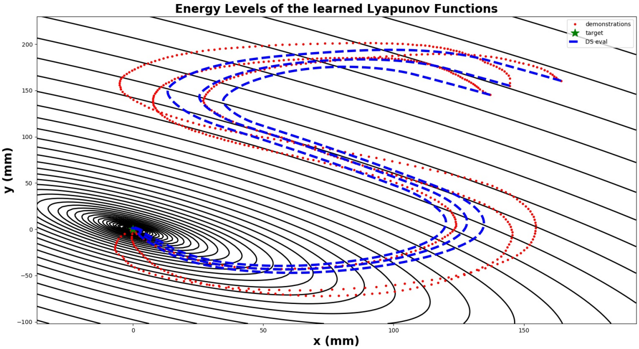

A CLF motion executor (red curves) that shows convergence to local attractors (green asterisks) and follows 3 different set trajectories (blue curves) for 2D nonlinear motion-trajectory problems on the WAM robot [Reproduced from Ogunmolu et al. (2020)].

Reproducing a Nonlinear Motion with GMM

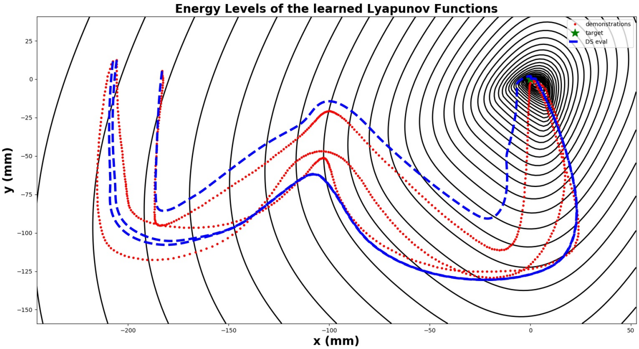

A CLF motion executor (red curves) that shows convergence to local attractors (green asterisks) and follows 3 different set trajectories (blue curves) for 2D nonlinear motion-trajectory problems on the WAM robot [Reproduced from Ogunmolu et al. (2020)].

Conclusions

- Designed a non-invasive soft robot for head motion compensation in IMRT/emerging MRI-LINACs ✓
- Photons-transparent; Adaptible under MRI coils for newer MRI-LINACs ✓
- Fast inference of beam orientations in treatment planning: Approx 60 secs beams prediction time✓
- Adapted H-∞ control methods for quantifying the brittleness of deep policies✓
- Devised a min-max-trained deep saddle policy for mitigating model mismatch, transfer errors, and policy sensitivity e.t.c. ✓

Publications

Johannes Heinrich, Marc Lanctot, and David Silver. Fictitious self-play in extensive-form games. In *International Conference on Machine Learning*, pages 805–813, 2015.

Sadeghnejad Barkousaraie, Azar and Ogunmolu, Olalekan and Jiang, Steve and Nguyen, Dan. A Fast Deep Learning Approach for Beam Orientation Selection Using Supervised Learning with Column Generation on IMRT Prostate Cancer Patients. *Medical Physics, American Association of Physicists in Medicine*, 2019.

Radhini Chelvarajah, Brigid Leighton, Linda Martin, Wayne Smith, and Rachael Beldham-Collins. Cranial immobilisation—is there a better way? *Radiographer*, 51(1):29–33, 2004.

Xinmin Liu, Andrew H Belcher, Zachary Grelewicz, and Rodney D Wiersma. Robotic stage for head motion correction in stereotactic radiosurgery. In *2015 American Control Conference (ACC)*, pages 5776–5781. IEEE, 2015.

Andrew Belcher. *Patient Motion Management with 6-DOF Robotics for Frameless and Maskless Stereotactic Radiosurgery*. PhD thesis, The University of Chicago, 2017.

Olalekan Ogunmolu and Rodney Wiersma. A Real-Time Patient Head Motion Correction Mechanism for MRI-Linac Systems. In *Joint AAPM | COMP Meeting, Virtual*, 2020.

James Pikul, Itai Cohen, and Robert Shepherd. Stretchable surfaces with programmable texture, May 2 2019. US Patent App. 16/161,029.

PC Parks. Liapunov Redesign of Model Reference Adaptive Control Systems. *IEEE Transactions on Automatic Control*, 11(3):362–367, 1966.

Olalekan Ogunmolu, Nicholas Gans, and Tyler Summers. Minimax Iterative Dynamic Game : Application to Nonlinear Robot Control. *IEEE International Conference on Intelligent Robots and Systems*, 2018.

Randy A Freeman and Petar V Kokotovic. Inverse optimality in robust stabilization. *SIAM journal on control and optimization*, 34(4):1365–1391, 1996.

S Mohammad Khansari-Zadeh and Aude Billard. Learning control Lyapunov function to ensure stability of dynamical system-based robot reaching motions. *Robotics and Autonomous Systems*, 62(6):752–765, 2014.

Olalekan Ogunmolu, Rachel Skye Thompson, and Rodrigo Pérez Dattari. Learning Control Lyapunov Functions in Python. `https://github.com/lakehanne/lyapunovearner`, 2020. Accessed February 10, 2020.

Olalekan Ogunmolu, Adwait Kulkarni, Yonas Tadesse, Xuejun Gu, Steve Jiang, and Nicholas Gans.

BOO: Search

- Formulated as a bandit search that imposes a regret term on the Q-value
- During the planning process, we estimate a *value*, $v(\mathbf{y}_t)$, that estimates the optimality of a beam block;
- In parallel, we refine the deep neural network policy by optimizing its weight in a separate thread.
  - Network parameters updated by a **mixed strategy** which combines its **pure strategy**,
  - It is a best response to the fictitious opponent's **average pure strategy**.

- Q-value defined as

$$\bar{Q}(s, a) = Q_j(s, a) + c\sqrt{\frac{2 \ln n(s)}{N(s, a}}, \tag{2}$$

$$a^\star = \arg\max_a \bar{Q}(s, a) \tag{3}$$

Fluence Map Optimization

- $\mathcal{X} \implies$ total discretized voxels of interest (VOI's) in a target volume
- $\mathcal{B}_1 \cup \mathcal{B}_2 \cup \ldots \cup \mathcal{B}_n \subseteq \mathcal{B} \implies$ beam partition subset
- $\mathcal{D}_{ij}(\theta_k) \implies$ matrix that describes each dose influence, d_i
  - delivered to a discretized voxel, i, in a volume of interest, VOI_h ($h = 1, \ldots, \mathcal{X}$), from a beam angle, θ_k, $k \in \{1, \ldots, n\}$

BOO: Fluence Map Optimization

- Suppose further that $\mathcal{D}_{ij}(\theta_k)$ is the matrix that describes each dose influence, d_i
    - delivered to a discretized voxel, i, in a volume of interest, $VOI_h \, (h = 1, \ldots, \mathcal{X})$, from a beam angle, θ_k, $k \in \{1, \ldots, n\}$
- We compute the matrix $\mathcal{D}_{ij}(\theta_k)$ by calculating each d_i for every bixel, j, at every φ°, resolution, where $j \in \mathcal{B}_k$

BOO: FMO problem definition

- The fluence problem is to find the values of decision variables, x_j, for which d_i to the tumor is maximized, while simultaneously minimizing the d_i to critical structures
- For the voxels in a target volume,
  - let a weighted quadratic objective minimize the l_2 distance between a pre-calculated dose $\boldsymbol{Ax}$, and a doctor's prescribed dose, $\mathbf{b}$
  - let a weighted quadratic objective maximizes the l_2 distance between $\boldsymbol{Ax}$ (where $\boldsymbol{x}$ represents the vectorized bixels, x_j) and $\mathbf{b}$

BOO: FMO problem definition

- Cost

$$\frac{1}{v_s} \sum_{s \in \text{OARs}} \|(b_s - \underline{w}_s \mathcal{D}_{ij}^s \boldsymbol{x}_s)_+\|_2^2 + \frac{1}{v_s} \sum_{s \in \text{PTVs}} \|(\bar{w}_s \mathcal{D}_{ij}^s \boldsymbol{x}_s - b_s)_+\|_2^2 \tag{4}$$

- Pre-calculated dose term: $\boldsymbol{Ax} = \{\sum_s \frac{w_s}{v_s} \mathcal{D}_{ij}^s \boldsymbol{x}_s \,|\, \mathcal{D}_{ij} \in \mathbb{R}^{n \times l}, n > l\}$, which is a combination of the dose components that belong to OARs and those that belong to PTVs.
- Let $w_s = \{\underline{w}_s, \bar{w}_s\}$ be the respective underdosing and overdosing weights for the OARs and PTVs
  - v_s represents the total number of voxels in each structure.

BOO: FMO

- Rewriting the objective

$$\min \frac{1}{2}\|A\mathbf{x} - \mathbf{b}\|_2^2 \quad \text{subject to } x \geq 0.$$

- With Lagrangian:

$$L(\boldsymbol{x}, \boldsymbol{\lambda}) = \min \frac{1}{2}\|A\mathbf{x} - \mathbf{b}\|_2^2 - \boldsymbol{\lambda}^T \boldsymbol{x}.$$

- Introducing an auxiliary variable $\mathbf{z}$, we have

$$\min_{\boldsymbol{x}} \frac{1}{2}\|\boldsymbol{A}\boldsymbol{x} - \mathbf{b}\|_2^2, \quad \text{subject to } \boldsymbol{z} = \boldsymbol{x}, \;\; \boldsymbol{z} \geq 0,$$

BOO: FMO by way of ADMM

- Solving either the $\boldsymbol{x}$ and $\boldsymbol{z}$ sub-problems, we have

$$\boldsymbol{x}^{k+1} = \left(\boldsymbol{A}^T\boldsymbol{A} + \rho\boldsymbol{I}\right)^{-1}\left(\boldsymbol{A}^T\boldsymbol{b} + \rho\boldsymbol{z}^k - \boldsymbol{\lambda}^k\right). \tag{5}$$

- And using the soft-thresholding operator, $S_{\boldsymbol{\lambda}/\rho}$, we find that

$$\boldsymbol{z}^{k+1} = S_{\boldsymbol{\lambda}/\rho}\left(\boldsymbol{x}^{k+1} + \boldsymbol{\lambda}^k\right), \tag{6}$$

where $S_{\boldsymbol{\lambda}/\rho}(\tau) = (x - \boldsymbol{\lambda}/\rho)_+ - (-\tau - \boldsymbol{\lambda}/\rho)_+$. $\boldsymbol{\lambda}$ is updated as

$$\boldsymbol{\lambda}^{k+1} = \boldsymbol{\lambda}^k - \gamma(\boldsymbol{z}^{k+1} - \boldsymbol{x}^{k+1}), \tag{7}$$

where γ is a parameter that controls the step length.

App A: 3-DOF Closed-loop Control

Closed-loop Phantom motion control along 3 DoFs with an adaptive neuro-controller.

3-DOF Simulation Testbed

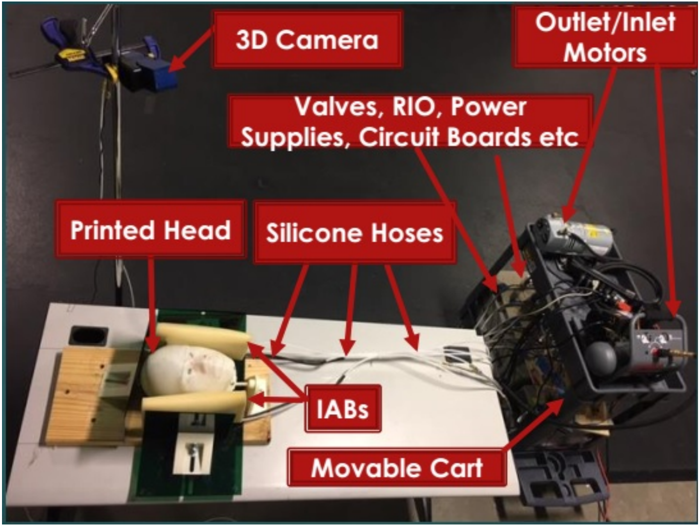

Hardware Description

Control Design Goals

- Stabilize z, pitch, and roll states, *i.e.*

$$\boldsymbol{x} = \begin{pmatrix} z \\ \theta \\ \phi \end{pmatrix}$$

- By solving an adaptive state feedback controller, optimal regulation, and minimize parametric uncertainties

Control Design Goals

- Provide closed loop tracking given a desired trajectory, **r**
- Robustify system to (non-)parametric uncertainties

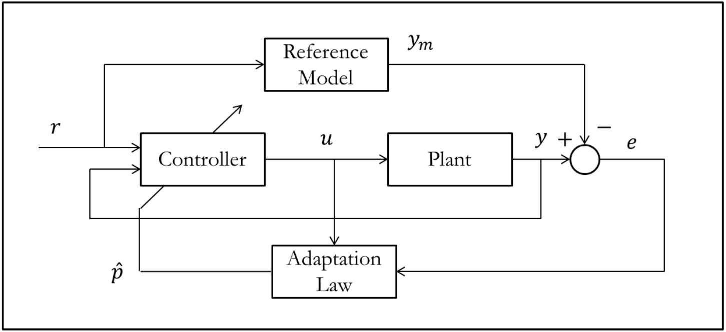

Indirect MRAC system. (Source mdpi.com)

Lyapunov Redesign: Theorem

- For correct adaptive gains, $\hat{\mathbf{K}}_x$ and $\hat{\mathbf{K}}_r$, $\mathbf{e}(k)$ is ***uniformly ultimately bounded***, and the state $\boldsymbol{x}$ converges to a neighborhood of $\mathbf{r}$.
- Choose a $\mathbf{V}$ in terms of $\mathbf{e}$; $\tilde{\mathbf{K}}_x^T$, $\tilde{\mathbf{K}}_r^T$; and parameter error $\varepsilon_f(\boldsymbol{x}(k))$ space

$$\mathbf{V}(\mathbf{e}, \tilde{\mathbf{K}}_x, \tilde{\mathbf{K}}_r^T) = \mathbf{e}^T\mathbf{P}\mathbf{e} + \mathbf{tr}(\tilde{\mathbf{K}}_x^T \boldsymbol{\Gamma}_x^{-1} \tilde{\mathbf{K}}_x^T |\boldsymbol{\Lambda}|) + \mathbf{tr}(\tilde{\mathbf{K}}_r^T \Gamma_r^{-1} \tilde{\mathbf{K}}_r |\boldsymbol{\Lambda}|)$$

Stability proof

$$\dot{\mathbf{V}}(\mathbf{e}, \tilde{\mathbf{K}}_y, \tilde{\mathbf{K}}_r) = \dot{\mathbf{e}}^T \mathbf{P}\mathbf{e} + \mathbf{e}^T \mathbf{P}\dot{\mathbf{e}} + 2\mathbf{tr}(\tilde{\mathbf{K}}_y^T \boldsymbol{\Gamma}_{\boldsymbol{y}}^{-1} \dot{\hat{\mathbf{K}}}_y |\boldsymbol{\Lambda}|) \\ + 2\mathbf{tr}(\tilde{\mathbf{K}}_r^T \boldsymbol{\Gamma}_r^{-1} \dot{\hat{\mathbf{K}}}_r |\boldsymbol{\Lambda}|)$$

$$= \left[\mathbf{A}_m \mathbf{e} + \mathbf{B}\boldsymbol{\Lambda}[\Delta\hat{\mathbf{K}}_r^T \mathbf{r} + \Delta\hat{\mathbf{K}}_x^T \mathbf{x}]\right]^T \mathbf{P}\mathbf{e} + \ldots \\ \mathbf{e}^T \mathbf{P}\left[\mathbf{A}_m \mathbf{e} + \mathbf{B}\boldsymbol{\Lambda}[\Delta\hat{\mathbf{K}}_r^T \mathbf{r} + \Delta\hat{\mathbf{K}}_x^T \mathbf{x}]\right] + \ldots \\ 2\,\mathbf{tr}(\Delta\mathbf{K}_x^T \Gamma_x^{-1} \dot{\hat{K}}_x |\boldsymbol{\Lambda}|) + 2\,\mathbf{tr}(\Delta\mathbf{K}_r^T \Gamma_r^{-1} \dot{\hat{\mathbf{K}}}_r |\boldsymbol{\Lambda}|)$$

Stability Analysis

$$= \mathbf{e}^T(\mathbf{P}\,\mathbf{A}_m + \mathbf{A}_m^T\mathbf{P})\mathbf{e} + 2\mathbf{e}^T\mathbf{P}\mathbf{B}\boldsymbol{\Lambda}\left(\tilde{\mathbf{K}}_y^T\mathbf{y} + \tilde{\mathbf{K}}_r^T\mathbf{r}\right)$$
$$+2\,\mathbf{tr}\left(\tilde{\mathbf{K}}_y^T\boldsymbol{\Gamma}_{\mathbf{y}}^{-1}\dot{\hat{\mathbf{K}}}_y|\boldsymbol{\Lambda}|\right) + 2\,\mathbf{tr}\left(\tilde{\mathbf{K}}_r^T\boldsymbol{\Gamma}_r^{-1}\dot{\hat{\mathbf{K}}}_r|\boldsymbol{\Lambda}|\right)$$

$$= -\mathbf{e}^T\mathbf{Q}\mathbf{e} - 2\mathbf{e}^T\mathbf{P}\mathbf{B}\boldsymbol{\Lambda}\varepsilon_f(\mathbf{y}) + 2\mathbf{e}^T\mathbf{P}\mathbf{B}\boldsymbol{\Lambda}\tilde{\mathbf{K}}_y^T\mathbf{y}$$
$$+ 2\,\mathbf{tr}\left(\tilde{\mathbf{K}}_y^T\boldsymbol{\Gamma}_{\mathbf{y}}^{-1}\dot{\hat{\mathbf{K}}}_y\right) + 2\mathbf{e}^T\mathbf{P}\mathbf{B}\boldsymbol{\Lambda}\tilde{\mathbf{K}}_r^T\mathbf{r} + 2\,\mathbf{tr}\left(\Delta\mathbf{K}_r^T\boldsymbol{\Gamma}_r^{-1}\dot{\hat{\mathbf{K}}}_r\right)$$

Notice $x^T y = \mathbf{tr}\left(y\,x^T\right)$ from trace identity

Stability Analysis Cont'd

Therefore,

$$\begin{aligned}
\dot{\mathbf{V}}(\cdot) &= -\mathbf{e}^T\mathbf{Q}\mathbf{e} - 2\mathbf{e}^T\mathbf{P}\mathbf{B}\boldsymbol{\Lambda}\varepsilon_f \\
&\quad + 2\,\mathbf{tr}\left(\tilde{\mathbf{K}}_y^T(\boldsymbol{\Gamma}_{\boldsymbol{y}}^{-1}\dot{\hat{\mathbf{K}}}_y + \mathbf{y}\mathbf{e}^T\mathbf{P}\mathbf{B}\,sgn(\boldsymbol{\Lambda})\right)|\boldsymbol{\Lambda}| \\
&\quad + 2\,\mathbf{tr}\left(\tilde{\mathbf{K}}_r^T(\boldsymbol{\Gamma}_r^{-1}\dot{\hat{\mathbf{K}}}_r + \mathbf{r}\mathbf{e}^T\mathbf{P}\mathbf{B}\,sgn(\boldsymbol{\Lambda})\right)|\boldsymbol{\Lambda}|
\end{aligned}$$

where for a real-valued x, we have $x = \text{sgn}(x)|x|$.

- first two terms will be negative definite for all $\mathbf{e} \neq 0$
  - since $\mathbf{A}_m$ is Hurwitz
- other terms will be identically null if we choose the adaptation laws

$$\dot{\hat{\mathbf{K}}}_y = -\boldsymbol{\Gamma}_{\boldsymbol{y}}\mathbf{y}\mathbf{e}^T\mathbf{P}\,\mathbf{B}\text{sgn}(\boldsymbol{\Lambda}), \quad \dot{\hat{\mathbf{K}}}_r = -\boldsymbol{\Gamma}_r\mathbf{r}\mathbf{e}^T\mathbf{P}\,\mathbf{B}\,\text{sgn}(\boldsymbol{\Lambda})$$

Stability Results: Ogunmolu et al. (2017)

$$\begin{aligned}\dot{\mathbf{V}}(\cdot) &= -\mathbf{e}^T\mathbf{Q}\mathbf{e} - 2\mathbf{e}^T\mathbf{P}\mathbf{B}\boldsymbol{\Lambda}\varepsilon_f \\ &\le -\lambda_{low}\|\mathbf{e}\|^2 + 2\|\mathbf{e}\|\|\mathbf{P}\mathbf{B}\|\lambda_{high}(\boldsymbol{\Lambda})\varepsilon_{max}\end{aligned}$$

- $\{\lambda_{low}, \lambda_{high}\} \equiv$ min/max eigenvalues of Q and $\boldsymbol{\Lambda}$.
- $\dot{\mathbf{V}}(\cdot)$ is thus negative definite outside the compact set: $\chi = \left(\mathbf{e} : \|\mathbf{e}\| \le \frac{2\|\mathbf{P}\mathbf{B}\|\lambda_{high}(\boldsymbol{\Lambda})\varepsilon_{max}(\mathbf{y})}{\lambda_{low}(\mathbf{Q})}\right)$
  - *i.e.* **e** is **uniformly ultimately bounded**, or $\mathbf{y}(t) \to 0$ as $t \to \infty$.

Appendix C: 1-DOF Closed-Loop Control

Left blank intentionally

Head Pose Estimation: Sensor Fusion

Sensors' Noise Floor

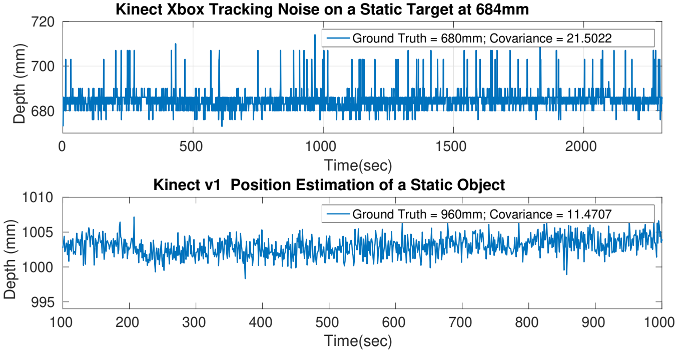

Case for Sensed Observation Filtering

Optimal head state estimation and sensor fusion

- Find the observation estimates $\hat{\mathbf{x}}(i)$ that minimize the mean-square error from true measurement, *i.e.* ,

$$\hat{\mathbf{x}}(i|j) = \arg \min_{\hat{\mathbf{x}}(i|j) \in \mathbb{R}^n} \mathbb{E}\{(\mathbf{x}(i) - \hat{\mathbf{x}})^T(\mathbf{x}(i) - \hat{\mathbf{x}})|z(1), \cdots, z(j)\}$$

- Define the estimate error's covariance as

$$\mathbf{P}(i|j) \triangleq \mathbb{E}\{(\mathbf{x}(i) - \hat{\mathbf{x}}(i|j))^T (\mathbf{x}(i) - \hat{\mathbf{x}}(i|j)) \,|Z^j\}. \qquad (8)$$

State estimation with Kalman filters

- Assume state model, $\mathbf{F}(k)$
- For a discretized time interval ΔT between measurements, we define the state

$$\mathbf{x}(k) = \mathbf{F}(k)\mathbf{x}(k-1) + \mathbf{B}(k)\mathbf{u}_k + \mathbf{G}_k\mathbf{w}_k \tag{9}$$

  - with

$$\mathbf{F} = \begin{bmatrix} 1 & \Delta T \\ 0 & 1 \end{bmatrix} \tag{10}$$

Kalman filters

- (9) $\implies \mathbf{x}_k = \mathbf{F}_k \mathbf{x}_{k-1} + \mathbf{G}_k \mathbf{w}_k$
- $\mathbf{G}_k :=$ uncontrolled forces accelerating on head
- Head's acceleration, $a_k \sim \mathcal{N}(0, \sigma_a)$
- Setting $\mathbf{G}_k = \mathbf{I}_{2x2}$ and $\mathbf{w}(k) \sim \mathcal{N}(0, \mathbf{Q}(k))$
  - set $\mathbf{Q}(k)$ to a random walk sequence, $\mathbf{W}_k = [\frac{\Delta T^2}{2}, \Delta T]^T$

Kalman Filters Design

- Such that

$$\mathbf{Q} = \mathbf{W}\mathbf{W}^T {\sigma_a}^2 = \begin{bmatrix} \frac{\Delta T^4}{4} & \frac{\Delta T^3}{2} \\ \frac{\Delta T^3}{2} & \Delta T^2 \end{bmatrix} {\sigma_a}^2. \tag{11}$$

- Set the transfer matrix from the estimates, $\mathbf{x}(k)$, to observations, $z_1(k)$ and $z_2(k)$ according to

$$z_s = \mathbf{H}_s(k)\mathbf{x}(k) + v_s(k) \qquad\qquad s = 1, 2 \tag{12}$$

  - where $\mathbf{H}_s(k) = \begin{bmatrix} 1, & 0 \end{bmatrix}^T$ and $v_s(k) \sim \mathcal{N}(0, \sigma_{rs}^2)$

KF Priori and Posteriori State Estimates

- **Prediction Phase:**

$$\begin{aligned} \hat{\mathbf{x}}_{k|k-1} &= \mathbf{F}\hat{\mathbf{x}}_{k-1|k-1} + \mathbf{B}_k\mathbf{u}_k \\ \mathbf{P}_{k|k-1} &= \mathbf{F}_k\mathbf{P}_{k-1|k-1}{\mathbf{F}_k}^T + \mathbf{Q}_k \end{aligned} \tag{13}$$

- **Update Phase:**

$$\begin{aligned} \mathbf{K}(k) &= \mathbf{P}(k|k-1)\mathbf{H}(k)^T[\mathbf{H}(k)\mathbf{P}(k|k-1)\mathbf{H}(k)^T + \mathbf{R}(k)]^{-1} \\ \hat{\mathbf{x}}(k|k) &= \hat{\mathbf{x}}(k|k-1) + \mathbf{K}(k)(\mathbf{z}(k) - \mathbf{H}(k)\hat{\mathbf{x}}(k|k-1)) \\ \mathbf{P}(k|k) &= (\mathbf{I} - \mathbf{K}(k)\mathbf{H}(k))\mathbf{P}(k|k-1) \end{aligned} \tag{14}$$

Xbox Filtering Results

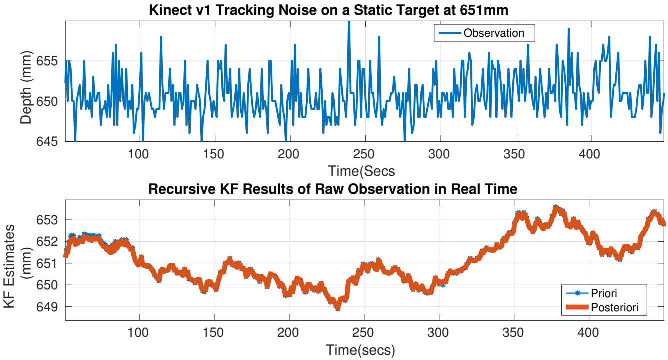

KF results of Xbox's observations

Kinect 2 Filtering Results

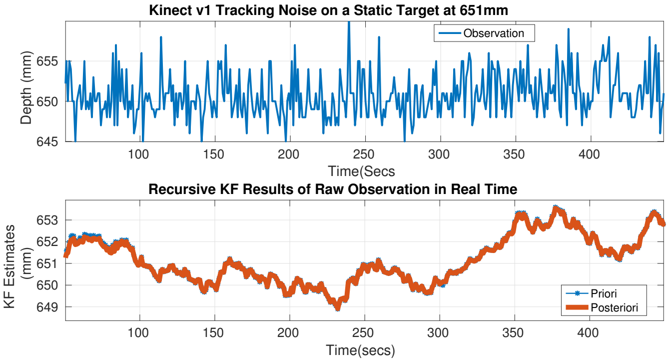

KF results of Kinect v1's observation

Filtering Results

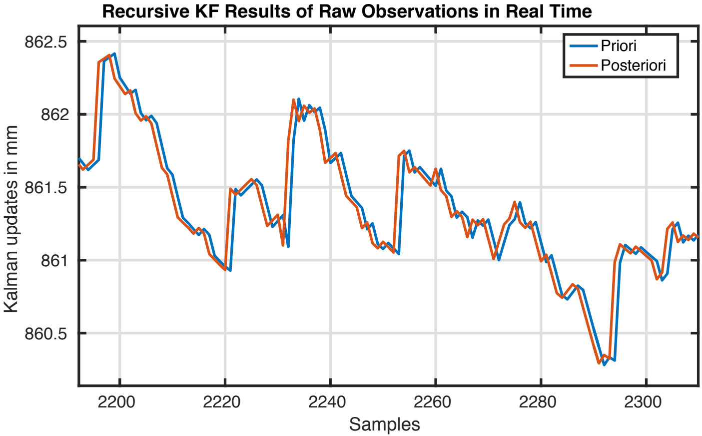

Global fusion of local tracks

- Fuse both updates with a variance-weighted average of each local track as follows,

$$\hat{\mathbf{x}}(F)(k|k) = \mathbf{P}(F)(k|k) \sum_{s=1}^{N} \left[\mathbf{P}(s)^{-1}(k|k)\hat{\mathbf{x}}(s)(k|k) \right]$$

$$\text{where } \mathbf{P}(F)(k|k) = \left[\sum_{s=1}^{N} \mathbf{P}(s)^{-1}(k|k) \right]^{-1}.$$

Track-to-track Fusion

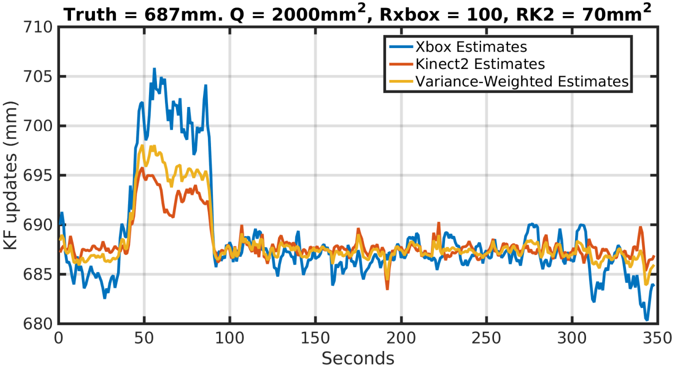

Track-to-track fusion of both sensors' local track estimates.

Vision-based Control

This page is left blank intentionally.

System Identification

- From I/O data, estimate a model
- Find set of optimal model parameters via the minimization,

$$G(t) = \arg \min_{\theta} V_N(\theta, Z^N)$$

  - where $V_N(\theta, Z^N) = \sum_{k=1}^{\mathcal{K}} \sum_{i=1}^{n} \frac{1}{2}(\hat{y}_i(k) - y_i(k))^2$,
  - and $Z^N = \{u(1) \cdots u(N),\ y(1) \cdots y(N)\}$
- After a least squares minimization, we derive a state-space realization,

$$\begin{aligned} \mathbf{x}(k + Ts) &= \mathbf{A}\mathbf{x}(k) + \mathbf{B}\mathbf{u}(k) + \mathbf{K}\mathbf{e}(k) \\ \mathbf{y}(k) &= \mathbf{C}\mathbf{x}(k) + \mathbf{D}\mathbf{u}(k) + \mathbf{e}(k) \end{aligned} \tag{15}$$

PID-PI Cascaded Controller

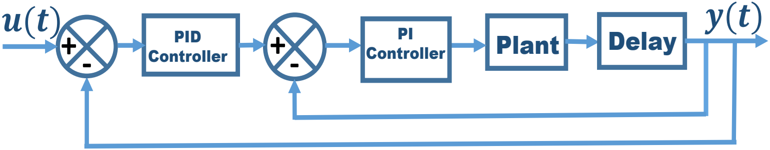

Open Loop Step Response

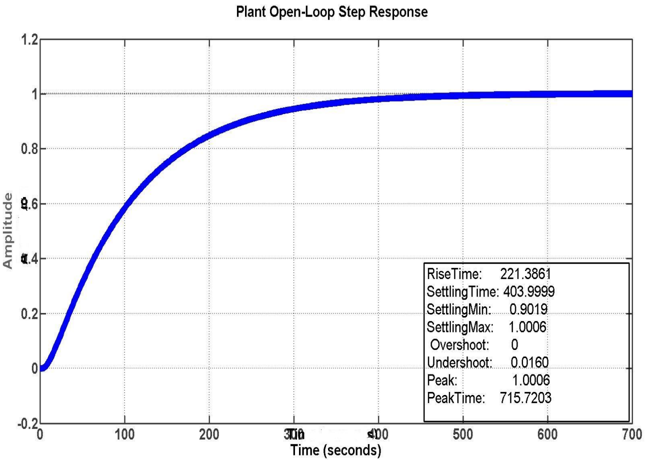

PI Closed-loop Step Response

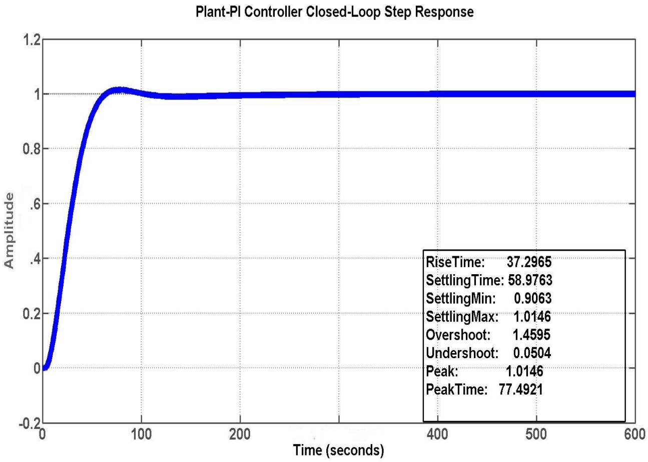

Cascaded PID-PI Closed-loop Step Response

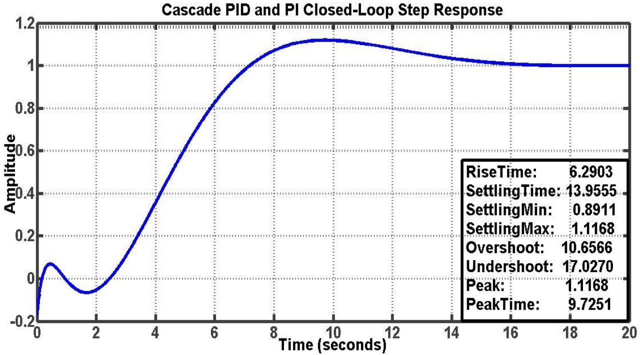

PI-PD Cascaded Controller Experimental Results

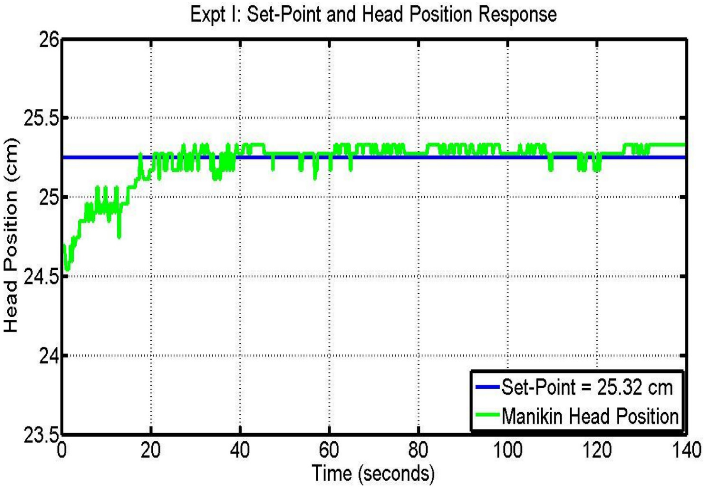

Varying Setpoint Simulation

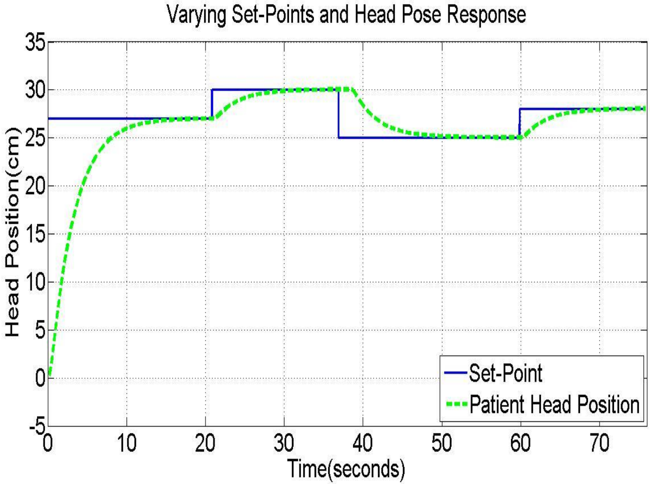

Varying Setpoint Experiment

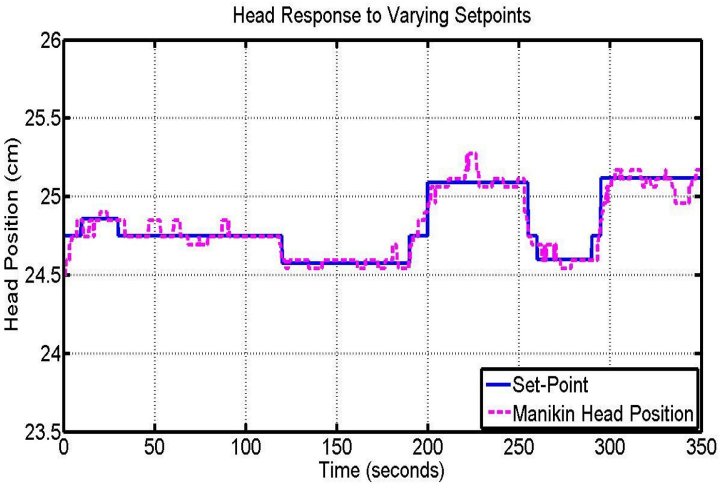

3-DOF Controller Design (IROS 2017)

- Posing the cost

$$J = \sum_{k=0}^{\mathcal{K}} x^T(k)\, Q\, x(k) + u(k)^T\, R\, u(k) + 2x(k)^T\, N\, u(k)$$

- we can obtain u as $\Delta u = \arg\min_{\Delta u} J$
- Δu is a future control sequence

Closed-loop control (Full state observer).

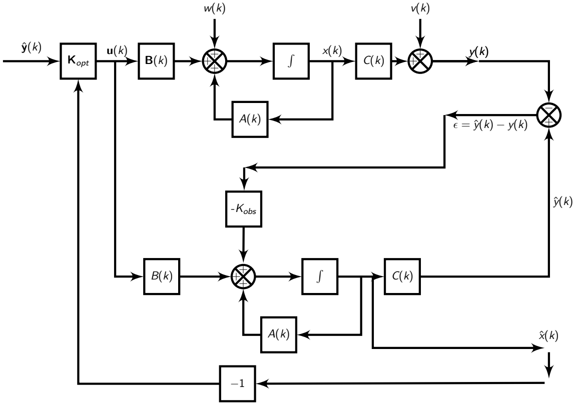

$$\hat{x}(k+1) = A(k)\hat{x}(k) - K_{obs}[C(k)\hat{x}(k) - y(k)] + B(k)u(k).$$

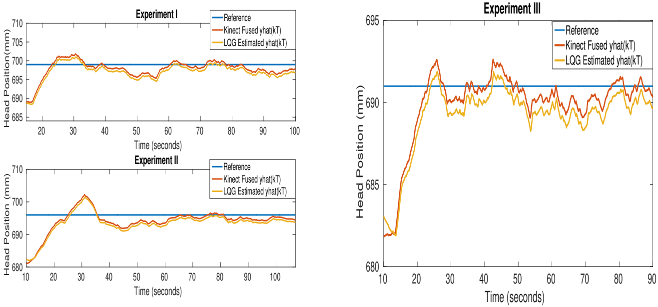

LQG Controller on mannequine head.

Appendix D: CCOARSE Actuator Schematic

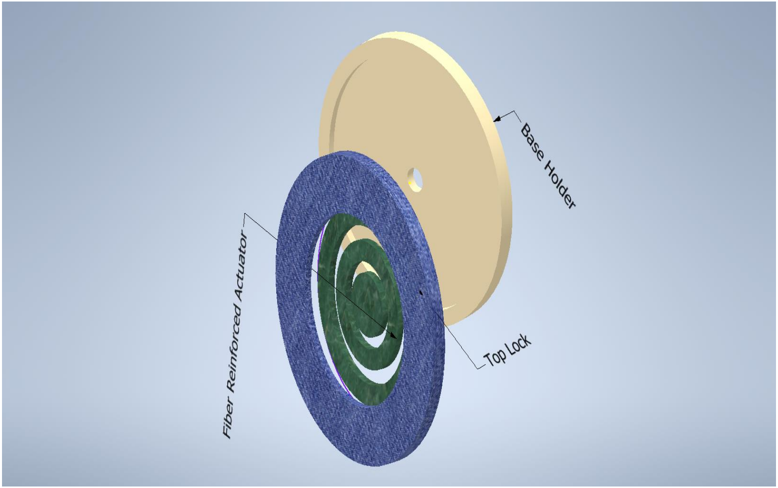

Soft IK via Boundary Value Problem

- With Cauchy's laws of motion, solve boundary volume problem of traction
  - Using the following boundary conditions for the Cauchy Stress,
    - $\sigma_{rr|R=R_0} = -P_{atm}, \sigma_{rr|R=R_i} = -P_{atm} - P$
  - And together with Cauchy's first law, we find that
    - $\sigma_{rr}(r) = -\int_{r_i}^{r_o}[2C_1(\frac{r}{R^2} - \frac{R^4}{r^5}) + 2\,C_2\left(\frac{r^3}{R^4} - \frac{R^2}{r^3}\right)]dr$
    - $\sigma_{rr}(r) = \int_{R_i}^{R_o}[2C_1\left(\frac{1}{r} - \frac{R^6}{r^7}\right) - 2C_2\left(\frac{R^4}{r^5} - \frac{r}{R^2}\right)]\,dr$
  - With $\sigma_{rr|R=R_i} = -P_{atm} - P$ and setting $P_{atm} = 0$, we find
    - $P(r) = \int_{r_i}^{r_o}[2C_1(\frac{r}{R^2} - \frac{R^4}{r^5}) + 2\,C_2\left(\frac{r^3}{R^4} - \frac{R^2}{r^3}\right)]dr$
    - $P(r) = \int_{R_i}^{R_o}[2C_1\left(\frac{1}{r} - \frac{R^6}{r^7}\right) - 2C_2\left(\frac{R^4}{r^5} - \frac{r}{R^2}\right)]\,dr$